

Resource-Efficient and Economically Viable Pyrometallurgical Processing of Industrial Ferrous By-products

Efthymios Balomenos · Ioanna Giannopoulou ·
Dimitrios Gerogiorgis · Dimitrios Panias ·
Ioannis Paspaliaris

Received: 24 July 2013 / Accepted: 14 November 2013
© Springer Science+Business Media Dordrecht 2013

Abstract This work outlines an integrated methodology for converting metallurgical by-products into high added value products, through an essentially zero-waste process. Thermodynamic modelling and conceptual design for processing bauxite residues (red mud) from the primary aluminium industry and ferro-nickel production slags are presented as examples. Furthermore, results of semi-industrial scale experiments for processing bauxite residues are illustrated, along with a preliminary financial analysis and an exergy flowsheet of the new conceptual alumina refinery, all confirming the financial viability as well as the resource-efficient utilization of the proposed technology.

Keywords Industrial by-products · Bauxite residues · Red mud · Slag · Pyrometallurgy · Mineral wool · Exergy efficiency

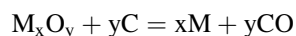
Introduction

The Greek primary metallurgical production is dominated by two major industries, namely the alumina refinery and aluminium production plant of Aluminium of Greece (AoG) and the ferro-nickel plant of LARCO. Both plants rely on unique Greek bauxite and laterite deposits, respectively, and both are owned exclusively by the Greek private (AoG) or state-owned (LARCO) sector. Today, both industries face significant challenges with respect to

handling and disposing of their by-products. Both the bauxite residue slurry (red mud) produced during alumina refining and the Fe–Ni slag produced during reductive EAF smelting represent key by-products generated in large amounts: 0.8 t of bauxite residues per tonne of metallurgical alumina and 14 t of Fe–Ni slag per tonne of Fe–Ni alloy on a dry basis, respectively. The annual by-product accumulation amounts to 650,000 t of bauxite residue and 2 million tonnes of Fe–Ni slag, on a dry basis. A strategic research priority of the Laboratory of Metallurgy at NTUA is the development of innovative technologies which will allow the efficient and sustainable valorisation of both by-products.

Thermodynamic Considerations

The chemical similarity between the bauxite residue and the Fe–Ni slag is illustrated in Table 1, which presents their average chemical analysis. In both cases, iron oxides represent 40 wt% or more of the by-product. A basic thermodynamic analysis of the Ellingham diagram for both systems (Fig. 1) reveals that carbothermic reductive smelting of both materials at temperatures between 1,400 and 1,600 °C would reduce the Fe, Cr, Ni, V and Na oxides to their metallic states, according to the general reaction:

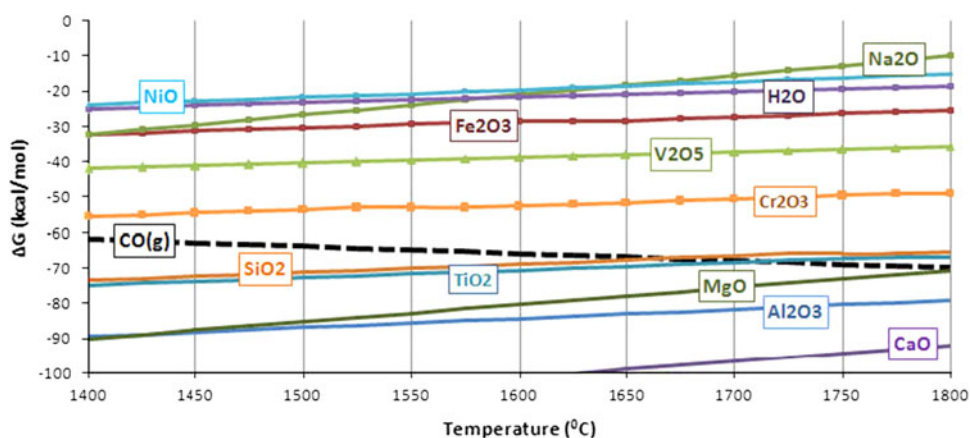


Metallic iron is liquid at 1,538 °C; in the presence of carbon, a binary eutectic system is formed (pig iron) which is liquid from as low as 1,154 °C (ledeburite eutectic point). Therefore, at thermodynamic equilibrium, carbothermic reductive smelting of both by-products above 1,400 °C would produce a pig iron metal phase in which V,

E. Balomenos (✉) · I. Giannopoulou · D. Gerogiorgis ·
D. Panias · I. Paspaliaris
Laboratory of Metallurgy, School of Mining and Metallurgical
Engineering, National Technical University of Athens (NTUA),
15780 Athens, Greece
e-mail: thymis@metal.ntua.gr

Table 1 Average chemical composition of bauxite residue from the Aluminium of Greece (ALSA) plant and Fe–Ni slag from the LARCO Fe–Ni plant

Bauxite residues	Al ₂ O ₃	CaO	SiO ₂	TiO ₂	Fe ₂ O ₃	Na ₂ O	V ₂ O ₅	LOI
(wt%)	16.22	10.73	6.08	5.93	47.74	2.51	0.21	10.42
Fe–Ni slag	Al ₂ O ₃	CaO	SiO ₂	MgO	Fe ₂ O ₃	Cr ₂ O ₃	NiO	LOI
(wt%)	9.69	3.47	38.27	5.13	39.78	2.47	0.10	0.95

Fig. 1 Ellingham diagram for the reduction of various oxides between 1,400 and 1,800 °C at atmospheric pressure. All reactions have been normalised to 0.5 oxygen mole production. Metal oxides above the CO(g) line are thermodynamically fully reduced by carbon at the given temperature (calculated by HSC Chemistry 6 software)

Ni and Cr would also be dissolved.¹ At temperatures around 1,600 °C, Si and Ti may also be reduced to a small extent, as the respective metals dissolved in the pig iron phase may have lower activities than the pure ones. The pig iron produced in this way can be sold directly to the secondary steel industry as a scrap substitute.²

The oxides which are not thermodynamically reducible by carbon at this temperature (1,600 °C) will form a slag phase, which in both cases amounts to at least 50 % of the initial by-product weight; 90 % of this slag weight consists of Al₂O₃-SiO₂-CaO oxides. A truly sustainable solution for managing these industrial by-products must be environmentally, economically and socially acceptable: therefore, it is imperative that such slag phases are *fully* transformed into marketable products. The latter may include mineral wool insulation products, cement additives, geopolymer products and other structured inorganic materials of reasonably high added value.

Therefore, the key objective of the envisioned by-product treatment process is to achieve the production of both high quality pig iron and slag products in a single step, by optimisation and adjustment of process conditions (e.g.

smelting temperature, amount of carbon used and flux additions). Temperature and carbon directly affect the extent of reduction reactions and thus control the distribution of elements between slag and pig iron phases. Fluxes such as silica sand and burnt lime primarily regulate slag phase composition, directly affecting its physico-chemical attributes (e.g. liquidus/solidus temperatures, viscosity, surface tension). Traditional pyrometallurgy uses fluxes in order to enhance metal production and operational conditions, achieving low temperature melts, good phase separation, pig iron desulfurisation and furnace refractory protection. In the context of the novel by-product process sought, fluxes are used both to optimise operational conditions as well as to achieve the production of a specifically designed slag phase.

The ENEXAL Bauxite Residue Treatment Process

Process Conceptual Design

The proposed bauxite residue treatment comprises four stages as shown schematically in Fig. 2. The first stage is the residue drying stage, necessitated by the high remaining moisture content of residues (up 25 % w/w), even when the best available upstream technology (filter press drying) is used for bauxite residue handling. This stage could occur in a double skin rotary kiln, using the heat content of the EAF hot off-gases or using waste heat from the alumina refinery itself (i.e. spent steam from the Bayer process). The second

¹ Metallic Na is gaseous above 883 °C and thus cannot be found in pig iron. Furthermore, it must be emphasised that carbothermic reduction of sodium oxide is thermodynamically impossible at this temperature when the substance is part of sodium-aluminosilicate phases (as in red mud). V, Ni and Cr on the other hand do not form aluminosilicate phases and are thermodynamically expected to be fully reduced.

² Pig iron scrap is currently valued at 400 €/t.

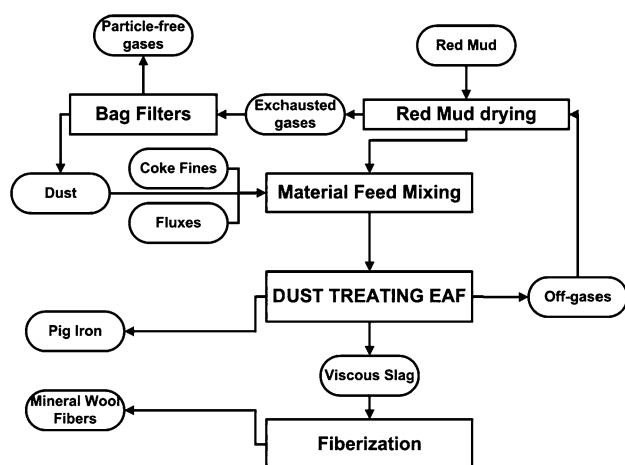


Fig. 2 The envisioned ENEXAL bauxite residue treatment process

stage of the process focuses on EAF feed material preparation: dried bauxite residue, coke fines and appropriate fluxes are mixed in order to adjust the properties of the produced slag. This mixture is fed into the EAF, where raw materials undergo reductive smelting and are transformed into three distinct fluid phases: liquid slag, liquid pig iron and off-gases. The off-gases after heat exchange in the bauxite residue dryer are sent to a bag-house unit to remove dust particles prior to releasing them to the atmosphere. The dust collected is recycled in the feed material. The liquid pig iron and slag phases are separated by sequential pouring (or by continuous tapping) and the liquid slag is fed directly to the final stage of the process, where it is fiberized to produce inorganic fibers and mineral wool products.

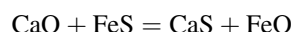
Mineral wool products are widely used as refractory, thermal and acoustic insulation or even construction materials due to their light weight, low thermal conductivity, incombustibility and high melting temperatures (>1,000 °C) [1]. In 2003 mineral and glass wool products accounted for 60 % of the thermoinsulation market in Europe [2]. Taking into consideration that in our case the EAF slag can be fiberized in situ, thus avoiding expensive melting of conventional mineral wool production (which accounts for up to 70 % of the total mineral wool production energy [3]), one can expect that the proposed bauxite residue treatment process is highly likely to be both economically viable and environmentally sustainable.

Thermodynamic Modelling

To prescribe process operating conditions and EAF parameters, product specifications must be considered and studied in detail. Typical chemical standards for pig iron steelmaking are: C = ~3–4 wt%, Si = 0.4–0.8 wt%, Mn = ~0.4 wt%, P = ~0.05 wt% and S < 0.02 wt%.

The melts used in typical mineral wool fiberisation process are liquid at 1,450 °C with viscosities of 10–15 P [4]. The chemical composition of such melts depends strongly on the raw material used (mineral, slag, glass) and the intended wool product use [5]. Slag wool contains SiO₂ (40–50 wt%), Al₂O₃ (10–20 wt%), CaO (10–40 wt%) and Fe₂O₃ (1–6 wt%); sodium, titanium and magnesium oxides may also be present.

To produce a pig iron metal phase of acceptably high quality by carbothermic reduction of bauxite residue, one must define the C:Fe atomic ratio in the feed material. A ratio of 1.5 corresponds to the stoichiometric ratio of carbothermic hematite reduction. However, since several side reactions occur (see Fig. 1) an excess of carbon is needed. The detailed thermodynamic model developed and preliminary inductive furnace lab-scale experiments reported previously by the authors [6] indicate that a C:Fe ratio of at least 2 is needed to achieve high iron recovery in the metal phase. Calcium oxide presence in the system is also important to prevent excessive sulphur presence in the pig iron, through the following desulfurisation reaction:



To produce a slag which can undergo efficient fiberisation, the slag phase of the system should be a stable liquid at 1,400 °C and must contain at least 60 wt% of SiO₂ and CaO combined. The phase diagram of the expected slag system has been calculated and visualised using FactSage[®]. As seen in Fig. 3, by adding a total of 350 kg of fluxes per tonne of bauxite residue processed, the resulting slag will have two liquid regions at 1,400 °C, one in a highly acidic region (slag basicity³: 0.2) and one in the nearly neutral region (slag basicity: 0.8–1.1). In order to protect furnace refractories and avoid excessive sulphur accumulation in the pig iron phase, the neutral region is selected.

Semi-industrial Scale EAF Experiments

To reliably establish optimal operating conditions, process experiments have been conducted using a semi-industrial scale (400 kVA) AMRT Electric Arc Furnace. The bauxite residue used was supplied by AoG and dried in a stationary electric dryer before being fed to the EAF. The optimal feed composition used was achieved by mixing 350 kg of dry bauxite residue with 77 kg of coke fines, 70 kg of silica and 54 kg of burnt lime. The C:Fe atomic ratio in the feed was thus set to 2.4 and the basicity ratio of the feed [(CaO + MgO)/SiO₂] was set to 0.94.

³ Slag basicity is defined here as the ratio of calcium and magnesium oxide mass sum to the mass of silicon oxides present in the slag melt.

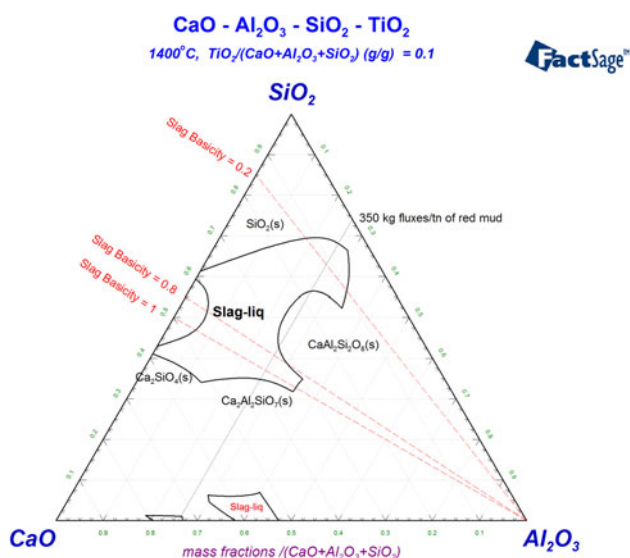


Fig. 3 Predicted triangular thermodynamic stability phase diagram for the liquid slag phase as predicted by FactSage[®] 6.3 software, for a system of varying CaO, Al₂O₃ and SiO₂ and constant TiO₂ composition [mass TiO₂/(mass CaO + mass Al₂O₃ + mass SiO₂) = 0.1; other bauxite residue slag oxides are omitted from the calculation] at 1,400 °C

Each batch experiment consisted of a furnace pre-heating stage (approximately 1 h long), followed by feeding of the raw material through a feeder tube at the top of the furnace, at a rate of approximately 3 kg/min (Fig. 4). The temperature on the surface of the melt produced was measured with an optical pyrometer at 1,540 °C (average value). In the end of batch feeding, two distinct phases were poured from the furnace (slag and pig iron): respective weight and chemical analysis data are presented in Table 2, along with thermodynamic model predictions for the same feed. It

must be noted that the Factsage thermodynamic model for this system, seems to overestimate the activity of Titanium in the liquid metal and predicts extensive reduction of TiO₂ oxide. This prediction is in complete disagreement with experimental results. In Table 2, empirical chemical composition indexes used in the mineral wool production industry are also presented to evaluate the fiberisation potential of the melt [7]. The latter show that the produced melt is well (or marginally) within empirical limits.

The pig iron chemical analysis shows that the metal produced has concentrated practically all the Fe and V content of the bauxite residue, as expected. Small amounts of Si and Ti metal have also been reduced therein. Sulfur (originating from bauxite residue as well as coke) and phosphorus (originating only from coke) were kept at minimum values, thus producing a metal phase which can be easily used in secondary steel production. Carbon content has the typical pig iron value (4 wt%). The chromium metal presence in the pig iron is not attributed to the feed material, but rather to magnesia-chromite refractory furnace lining, which was partially dissolved during the carbothermic reduction. The slag phase chemical analysis shows that Al, Si, Ca, Mg and Ti have remained as oxides in the slag phase, in an overall neutral melt (basicity ratio = 1.05), again as expected. The overall elemental distribution is shown in Fig. 5, where both the partial dissolution of the furnace lining and the partial evaporation (ca. 41 wt%) of Na content is apparent. The latter result is in agreement with previous experimental observations [6]. To avoid refractory dissolution a different refractory lining must be used in industrial production; initial tests with an Alumina–SiC brick refractory lining and slightly higher basicity slag ratios (i.e. 1.2) have shown significantly higher chemical stability.

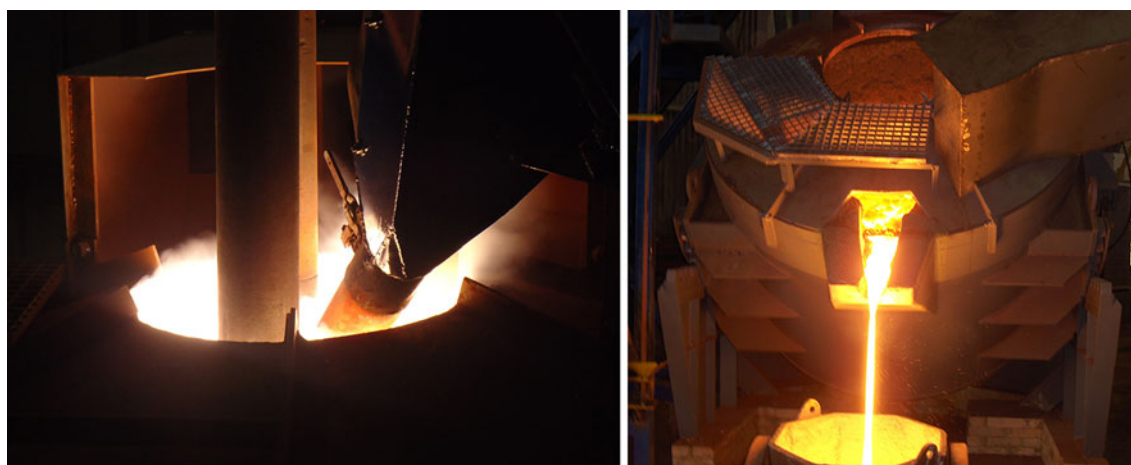


Fig. 4 Photos of the EAF during batch feeding (*left*) and during pouring (*right*)

Table 2 Thermodynamic model (FactSage[®] calculation: using databases FTmisc (solution Fe-liq) and FToxid (solution ASlag-liq), at 1,600 °C, and 1 bar total pressure, in absence of air) and experimental results from processing 350 kg of bauxite residue in a semi-industrial scale (400 kVA) EAF

Pig iron (wt%)	Model prediction	EAF exp	Slag (wt%)	Model prediction	EAF exp	Empirical indexes for mineral wool production	
%Fe	86.57	87.09	CaO	31.19	29.65	A [<1.8]	1.85
%C	4.67	4.05	SiO ₂	32.71	32.64	P [<15]	15.06
%S	0.16	0.05	Al ₂ O ₃	29.68	24.23	k2 [0.8–1]	0.76
%P	–	0.20	TiO ₂	1.97	6.78	SHG [1.3–1.4]	1.26
%Si	1.89	1.71	MgO	1.40	4.65	KNB [30–40]	36.19
%Ti	6.38	0.46	Na ₂ O	2.69	1.89	N [<5 %]	1.89
%V	0.29	0.28	Fe ₂ O ₃	0.05	1.11	F [>5 %]	1.11
%Cr	–	4.43	–SO ₃	0.57	1.09		
Total weight	124 kg	120 kg	Total weight	271 kg	280 kg		
Fe recovery	100 %	97 %	Slag basicity	0.99	1.05		

Empirical indexes (oxides in wt%) A = (SiO₂ + Al₂O₃ + TiO₂)/(CaO + MgO); N = 4.9/[(MgO + CaO + Fe₂O₃ + Na₂O + TiO₂)/(SiO₂ + Al₂O₃)] – 0.45; k2 = [100 – (SiO₂ + Al₂O₃)]/(SiO₂ + Al₂O₃); SHG = (SiO₂ + Al₂O₃)/(1.4 MgO + 0.4 Fe₂O₃ + CaO + TiO₂); KNB = Na₂O + MgO + CaO; N = Na₂O; F = Fe₂O₃

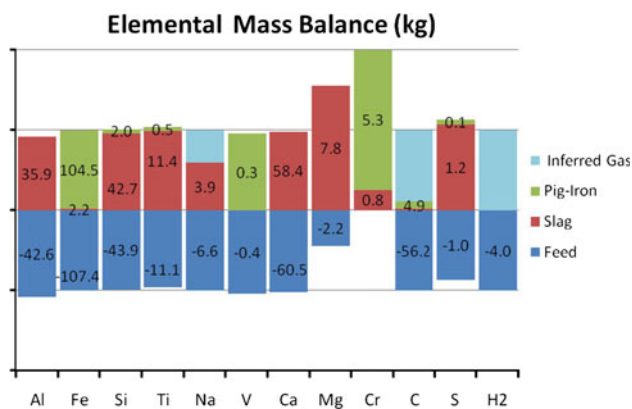


Fig. 5 Normalised elemental mass balance of batch feed and EAF smelting phases. Feed mass is represented by *negative values*, while pig iron, slag and inferred gas masses appear as *positive values*. Labels represent actual weight of respective elements in kg

Slag Fiberisation Tests

During slag phase pouring, part of the slag has been fiberised using a high-speed air/water jet positioned app 80 cm below the furnace top, as shown in Fig. 6 (left). The vertical distance of the air/water jet from the furnace top (tapping point) is of pivotal importance in this kind of fiberisation process, as evidenced by CFD model temperature results shown in Fig. 7 and described in detail elsewhere [8]. Temperature differences between the outer and inner layers of the vertical molten slag stream flow (at the level where the latter reaches the impingement point) will cause problems in the fiberisation process, especially if the melt is close to its solidification temperature.

The inorganic fibers produced from the slag during these preliminary experiments have been examined with

scanning electron microscopy (SEM), in order to quantitatively examine fiber physical properties and quality. As seen in Fig. 6 (right), most fibers formed have a diameter of less than 20 μm , along with the presence of some substantially thicker fibers. Commercial vitreous wool products have an average diameter of 3–10 μm while individual fibres may range from <1 to >20 μm .

While this test system employed to fiberize the slag has been processed at operating conditions far from their optimal values, experimental results prove that slag melts can be fiberised efficiently and uniform fibers can be produced, either by means of the proposed (melt blowing) process optimization or using established industrial (e.g. melt spinning) process automation.

Fiberisation Efficiency

Molten inorganic slag fiberization has a strong industrial potential which requires detailed study: in particular, melt-blowing plants can surpass the widely established melt-spinning technologies. For a fundamental quantitative understanding of the mineral fiberisation process, one must consider and use a dynamic mathematical model and use it to describe fiber formation [9]. A number of fundamental simplifying assumptions are required in order to accurately capture the essential state variables of each slag fiber while ensuring compact model size and manageability. The fundamental assumption is that molten slag droplet cooling and fiber elongation both occur without significantly altering the external air flow field and without any secondary phenomena. Primary slag jet breakup occurs swiftly and entirely within very limited space and time. Air jet impingement on slag establishes a known, normal initial slag droplet velocity

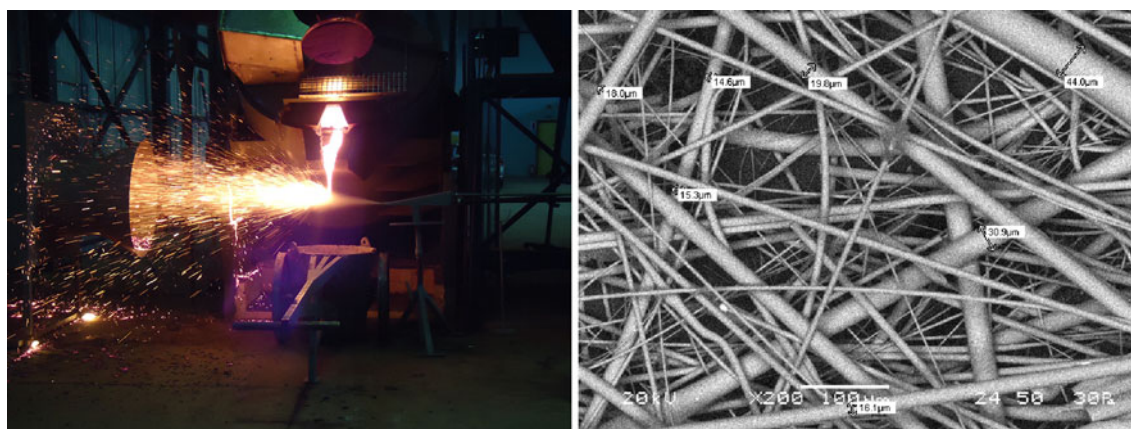


Fig. 6 Photograph of air/water jet slag fiberisation process (*left*); SEM photograph of inorganic fibers produced (*right*)

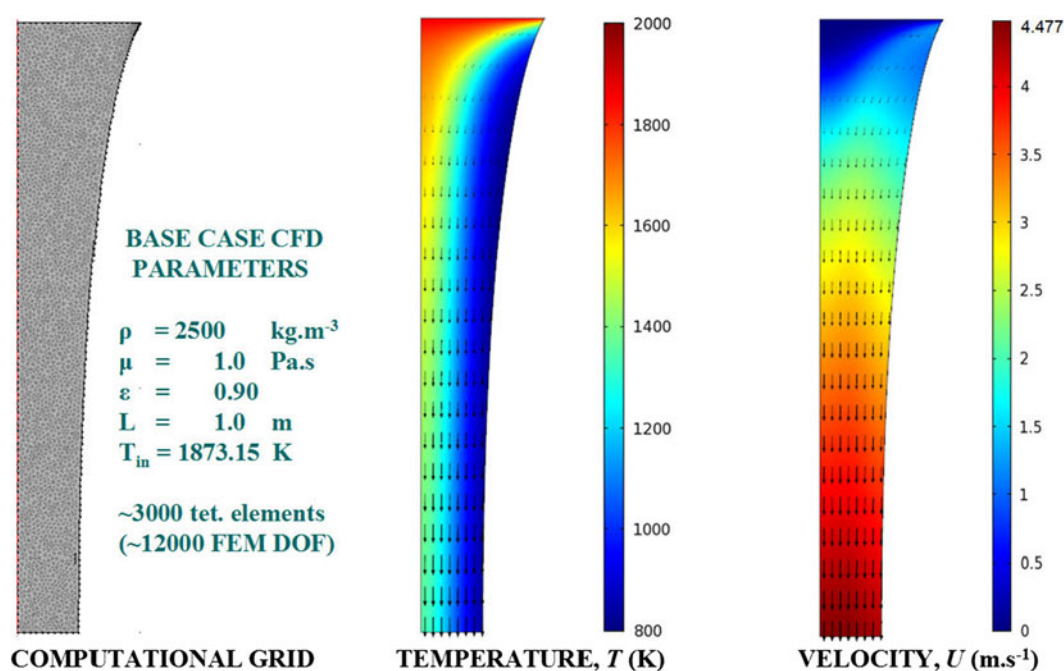


Fig. 7 Axisymmetric unstructured grid and indicative solution profiles for the nonisothermal flow problem of the slag melt from the furnace mouth to the level of the air/water jet level [8]

distribution as well as a known dispersion cone, whose apex is the initial position of all slag droplets at $t = 0$. Each spherical droplet remains an oblate ellipsoid which undergoes continuous transformation, with radius $r(t)$, length $L(t)$ and temperature $T(t)$ continuously varying under mass conservation. Mineral slag droplets and nascent fibers move unperturbed along independent flight trajectories; secondary breakup, collision, coagulation and agglomeration phenomena can be ignored. The number and total mass of the entire molten slag particle population hence remains constant.

Melt-blowing slag fiberisation is studied rigorously via an ODE system model in MATLAB[®], considering

unperturbed flight and simultaneous radiative cooling in a two-dimensional domain, assuming a normal initial slag droplet velocity distribution, $N(1, \sigma)v_{\text{mean}}$ (here, $v_{\text{mean}} = 5 \text{ m/s}$). A sensitivity analysis of fiber flight trajectory swarms as a function of dispersion cone angle as well as velocity standard deviation shows great variability in flight length and deposition width. Figure 8 illustrates mineral fiber flight trajectory swarms for 200 identical slag droplets ($r_0 = 5 \mu\text{m}$).

A sensitivity analysis of elongated fiber temperature and size as a function of initial droplet size has been performed in order to assess the importance of initial droplet size

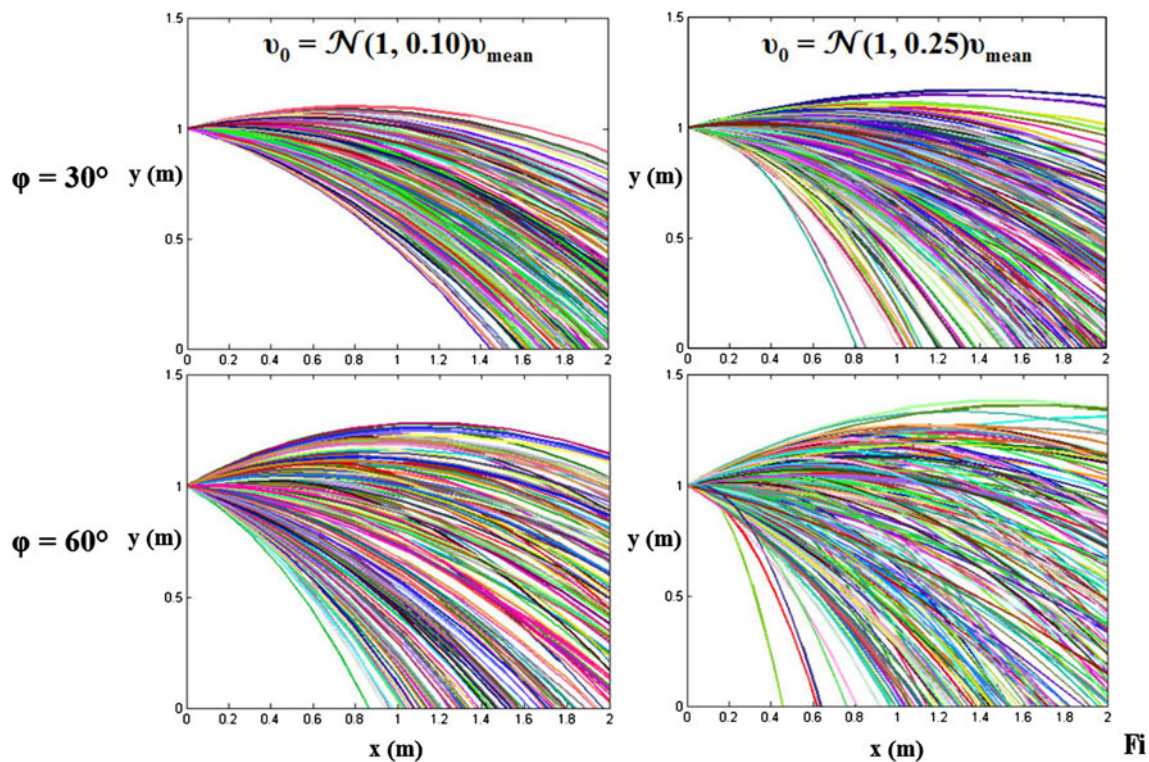


Fig. 8 Mineral fiber xy-trajectories for different dispersion cone angles and initial velocity distributions ($N = 200$ molten slag droplets)

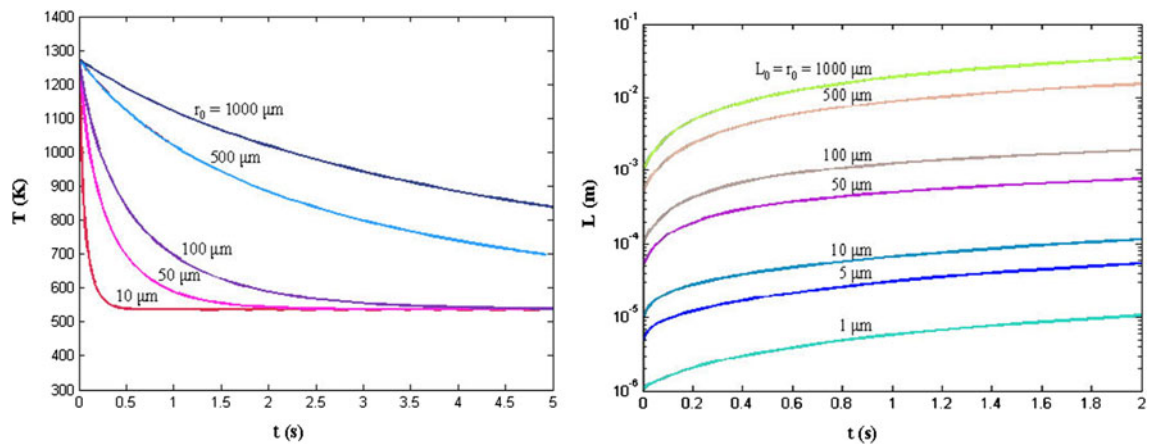


Fig. 9 Mineral fiber temperature (T) and elongation (L) as a function of time for different initial particle sizes

distribution (Zone 2). Figure 9 illustrates mineral fiber temperature and size evolution for various initial droplet sizes.

Model simulation results for nascent mineral fiber flight trajectories indicate that elongated fiber scattering metrics increase for increasing dispersion cone angle and (even more) for increasing standard deviation, thereby implying that achieving a narrow, well-formed conical droplet spray in the fiberisation zone is critical in order to avoid unacceptably short or long trajectories and prevent extreme product variability. Flexibility in positioning the collection chamber is thus key towards minimizing material losses.

Economic Viability

A vital aspect of the novel process, is its profitability potential with respect to the metallurgical and materials industry. By extrapolating the 400 kVA EAF results to a 5 MVA EAF processing 1,300 t of dry bauxite residue per month, production of 440 t of pig iron and 980 t of slag for fiberisation can be achieved. Taking into account the current cost of raw materials (other than bauxite residues), electrical energy and labour in Greece, the total operating cost of this unit is predicted at 766,217 € per month. Based

Fig. 10 Preliminary cost analysis (*left*) and profit margin analysis for different mineral wool prices (*right*) for a 5 MVA EAF process treating 1,300 t of bauxite residue per month

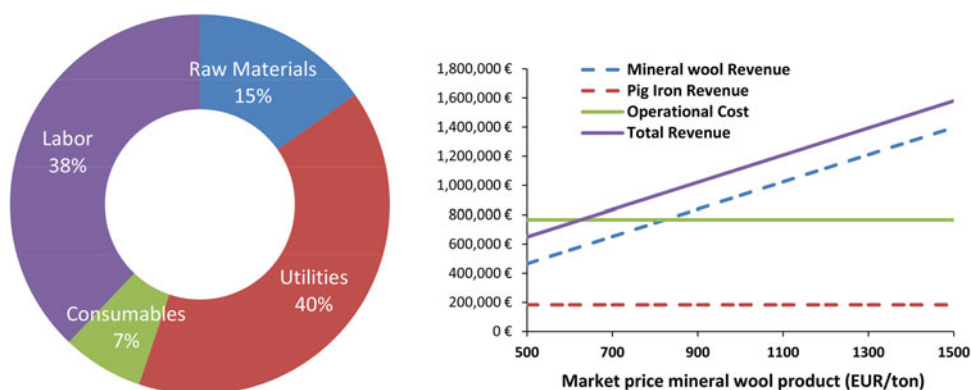
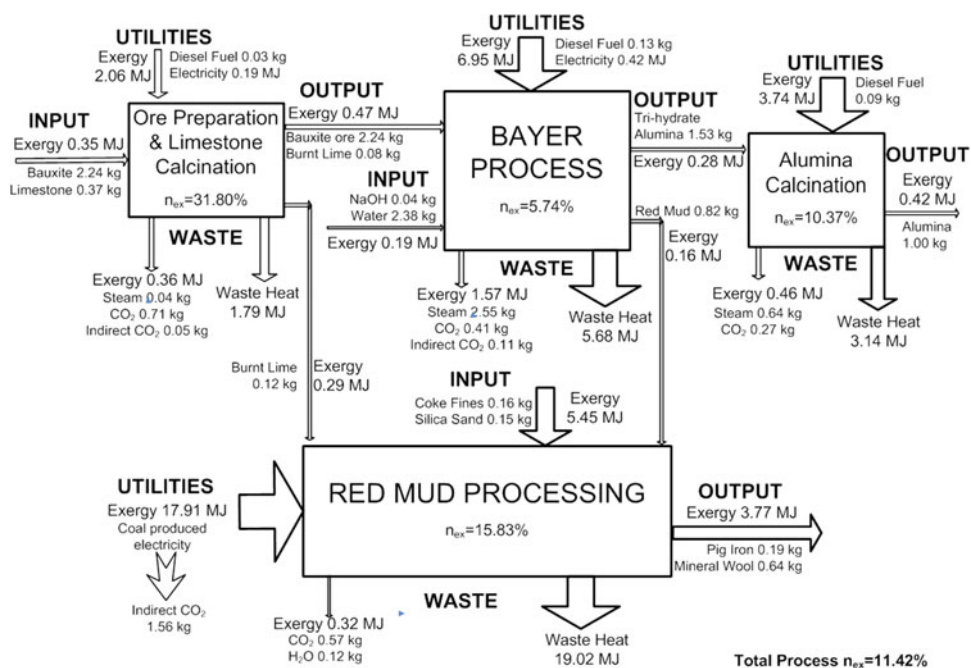


Fig. 11 The exergy analysis performed for the new alumina refinery



on current prices for pig iron scrap, selling the pig iron alone would only cover 25 % of the total operating cost. By adding the slag fiberisation stage, the overall operation would become viable if the mineral wool product can be sold at a minimum of 626 €/t (break-even price). Currently, commercial mineral wool product prices range in between 600 and 1,000 €/t. The results of this preliminary economic analysis are shown in Fig. 10. Yet this is still a very basic and preliminary analysis, as in order to process the 650,000 t of BR produced annually in AoG one would need significantly higher processing capacities (i.e. 20–40 MVA EAFs).

Resource Utilization Efficiency

Further to the economic viability of the process, it is equally important to examine its resource utilization

efficiency in order to assess and quantify the process contribution towards sustainable development. An important thermodynamic concept for such a calculation is *exergy*, which can be defined as the resource consumed by dissipative structures (e.g. chemical reactors) to remain in states far from thermodynamic equilibrium with their environment, or as the resource consumed by decaying structures as they proceed to thermodynamic equilibrium with their environment [10]. Exergy is measured in energy units, is always defined in relation to the environment of a given system and is divided according to its carrier flow into exergy of energy (heat and radiation) and exergy of matter (chemical and thermomechanical) [11]. Any industrial process related to extractive metallurgy can be defined as a process where matter with low chemical exergy (ore) is transformed into matter with high chemical exergy (metal, pure oxides) with the consumption of

exergy provided by utilities and chemical agents (fuel for heating, reducing agents). The exergy efficiency of the process (or the *resource utilization efficiency*) is then defined as the ratio of the exergy embodied in the final product to the exergy embodied in the initial ore, fluxes and utilities used in the process.

The authors have published [12] a detailed analysis of the primary aluminium industry which indicates the exergetic inefficiency of the Bayer process: the latter expends a large amount of exergy as heat in order to chemically separate aluminium oxides from the bauxite ore. The total Bayer process exergy efficiency is only 3.66 %.

By incorporating the bauxite residue treatment process (described in the previous section) into the flowsheet of a primary alumina refinery and calculating the respective exergy flows, a substantial improvement in the plant resource utilization efficiency is foreseen, as shown in Fig. 11. Details on exergy flow calculations are presented elsewhere [13].

Fe–Ni Slag Treatment

Using a similar methodology to the one described in “The ENEXAL Bauxite Residue Treatment Process” section, a process to treat Fe–Ni slag for the production of pig iron and high added value slag products can also be envisioned. The system chemistry is simpler and (due to the high SiO₂ content), only lime addition is needed as a flux to regulate the final slag melt basicity. The FactSage[®] phase diagram calculation for the system (Fig. 12) shows that a liquid slag can be produced at 1,400 °C for practically any slag basicity ratio. For the same reasons mentioned in the bauxite residue treatment section, the neutral slag region has been selected. FactSage[®] model predictions along with empirical melt composition indexes are presented in Table 3.

Using the same financial scenario as in the case of the bauxite residue treatment, this process implemented in a 5 MVA EAF would produce 403 t of pig iron and 1,100 t of fiberisable slag with an operating cost of 724,581 €/month. This in turn means that the break-even price for the mineral wool product could be as low as 533 €/t. Moreover, if the processing unit is set up within an existing Fe–Ni industrial plant, then the slag could be processed before cooling, thus tremendously reducing the energy and processing time needed in the 5 MVA EAF. Theoretically, a sevenfold increase in the amount of processed slag can be attained within the same time and with the same energy consumption, thus leading to an even lower break-even price of 429 €/t of mineral wool.

In contrast to the bauxite residue treatment process, the Fe–Ni slag process has not yet been tested at semi-

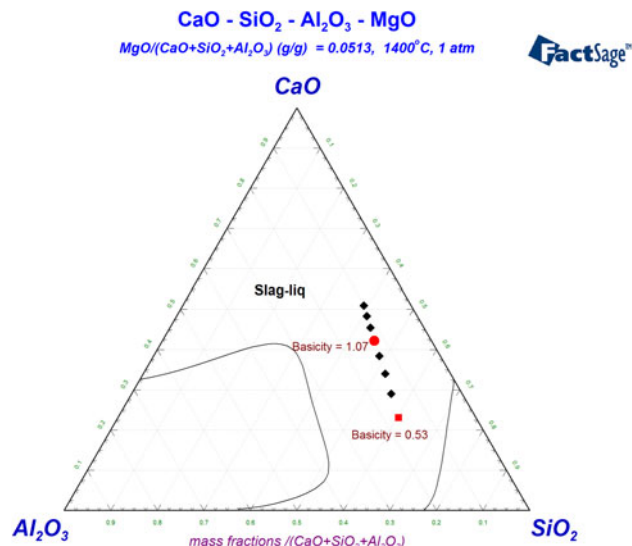


Fig. 12 Predicted triangular thermodynamic stability phase diagram for the liquid slag phase as predicted by FactSage[®] 6.3 software, for a system of varying CaO, Al₂O₃ and SiO₂; and constant MgO composition [mass TiO₂/(mass CaO + mass Al₂O₃ + mass SiO₂) = 0.0513; other Fe–Ni slag oxides are omitted from the calculation] at 1400 °C. The corresponding slag for different lime additions is shown with *bullets*. The *square* corresponds to the addition of 10 kg and the *circle* to the addition of 30 kg of CaO per 100 kg of Fe–Ni slag, respectively

Table 3 Predicted thermodynamic equilibrium composition of the phases produced during the processing of a 100 kg of Fe–Ni Slag with 30 kg of lime and 11 kg of carbon at 1,600 °C (FactSage[®] calculation: using databases FTmisc (solution Fe-liq) and FToxid (solution ASlag-liq), at 1,600 °C and 1 bar total pressure, in absence of air)

Pig iron (wt%)	Model	Slag (wt%)	Model	Empirical indexes for mineral wool production	
%Fe	89.49	Al ₂ O ₃	29.65	A [<1.8]	1.19
%C	1.98	CaO	32.64	P [<15]	12.45
%Cr	5.11	SiO ₂	24.23	k2 [0.8–1]	0.85
%Ni	0.25	MgO	6.78	SHG [1.3–1.4]	1.13
%Si	3.17	FeO	4.65	KNB [30–40]	45.60
		CrO	1.89	N [<5 %]	0.00
				F [>5 %]	0.08
Total weight	31.03 kg	Total weight	84.63		
Fe recovery	99.79 %	Slag basicity	1.07		

Cr remaining in the slag is expected to be present as Cr(II) or Cr(III) due to the highly reductive conditions imposed

industrial or industrial scale. Therefore, it is presented here only as a theoretical concept and requires further investigation.

Conclusions

A methodology for carbothermic treatment of ferrous slags and by-products (with $\text{Fe}_2\text{O}_3 \geq 40$ wt%) has been developed and tested at semi-industrial scale. The major strategic advantages of the novel process design include the complete exploitation and processing of the slag produced, the production of high added value materials and the potential for systematic determination of appropriate flux regulation. This work examines the case of considering mineral wool fiber production as an integral part of profitable and sustainable operation, for both bauxite residue and Fe–Ni slag treatment.

Numerous other slag products can also be produced with the use of appropriate fluxes. Calcium- and magnesium-bearing slags from blast furnaces have already been successfully used for producing geopolymers [14]. The latter can be used as cement additives, as insulation materials [15] or even as fire-proofing materials [16]. The development of numerous slag products is vital for the industrial application of the two processes described here, because the preliminary economic analysis clearly indicates that the overall process profitability strongly depends on efficient marketing and commercial exploitation of high added value slag products.

Experimental investigation of both proposed processes at industrial pilot scale is the obvious next step required, in order to demonstrate that there is clear potential for industrial implementation. Under the auspices of the FP7 ENEXAL project, a 1 MVA EAF pilot plant has thus already been set up within the Aluminium of Greece plant in order to perform long-term continuous testing of the bauxite residue treatment process.

Acknowledgments The research leading to these results has received funding from the European Union Seventh Framework Programme (FP7/2007–2013) under Grant Agreement No. ENER/FP7/249710/ENEXAL (www.labmet.ntua.gr/ENEXAL).

References

1. Fitzer, E. (ed.): Ullmann's Encyclopedia of Industrial Chemistry, Fibres, 5. Synthetic Inorganic. Wiley, Hoboken (2009)

2. Karamanos, A.K.: Comparative evaluation of stone wool and extruded polystyrene. Heleco'05, pp. 1–11 (in Greek) (2005)
3. IPPC: Integrated Pollution Prevention and Control Reference Document on Best Available Techniques in the Glass Manufacturing Industry. European Commission (2001). <http://eippcb.jrc.ec.europa.eu/reference/>
4. Blagojevic, B., Sirok, B.: Multiple regression model of mineral wool fibre thickness on a double-disc spinning machine. *Glass Technol* **43**(3), 120–124 (2002)
5. Ullmann's Encyclopedia of Industrial Chemistry, Chapter: Fiber, 5. Synthetic Inorganic, Wiley-VCH Verlag GmbH, KGaA, Weinheim, (2005). doi:10.1002/14356007
6. Balomenos, E., Giannopoulou, I., Pantias, D., Paspaliaris, I.: A novel red mud treatment process: process design and preliminary results. *Travaux ICSOBA* **36**(40), 255–266 (2011). (Edited and published by ICSOBA Secretariat Nagpur, India)
7. Information disclosed to author in private communications
8. Gerogiorgis, D., Pantias, D., Paspaliaris, I.: Multiphysics CFD modeling of a free falling jet during melt-blowing slag fiberisation. In: Nastac, L., Zhang, L., Thomas, B.G. et al. (eds.) *CFD Modeling and Simulation in Materials Processing*, pp. 81–88. Wiley, Hoboken (2012)
9. Gerogiorgis, D., Pantias, D., Paspaliaris, I.: Stochastic modeling and simulation of fiber evolution during melt-blowing slag fiberization. In: *Collected Proceedings of the TMS 2012 Annual Meeting (CD)*. TMS, Warrendale (2012)
10. Szargut, J.: International progress in second law analysis. *Energy* **5**, 709–718 (1980)
11. Brodyansky, V.M., et al.: *The Efficiency of Industrial Processes: Exergy Analysis and Optimization*. Elsevier Science, Amsterdam (1994)
12. Balomenos, E., Pantias, D., Paspaliaris, I.: Energy and exergy analysis of the primary aluminium production processes—a review on current and future sustainability. *Miner. Process. Extr. Metall. Rev.* **32**, 69–89 (2011)
13. Balomenos, E., Pantias, D., Paspaliaris, I., Kastiris, D., Boufonos, D.: Exergetic analysis of the ENEXAL bauxite residue treatment on the overall resource efficiency of the primary alumina refining process. *International Exergy, Life Cycle Assessment, and Sustainability Workshop and Symposium (ELCAS3)*, Proceedings, pp. 427–436 (2013)
14. Davidovits, J.: *Geopolymer Chemistry and Applications*, 2nd edn. Institut Géopolymère, Saint-Quentin (2008)
15. Maragos, I., Giannopoulou, I., Pantias, D.: Synthesis of ferromagnetic slag-based geopolymers. *Miner. Eng.* **22**, 196–203 (2008)
16. Sakkas, K., Nomikos, P., Sofianos, A., Pantias, D.: Inorganic polymeric materials for passive fire protection of underground constructions. *J. Fire Mater.* (2012). published online doi:10.1002/fam.2119